THE EFFECT OF FIBERS ON TURBULENT QUANTITIES IN BACKWARD FACING STEP CHANNEL FLOW: MEASUREMENTS AND NUMERICAL SIMULATIONS

Kati J. Lindroos
Mechanical Pulping Lines, Metso Paper Valkeakoski Oy
PO Box 125, FIN-37601 Valkeakoski, Finland
kati.lindroos@metso.com

Mika V. Piirto, Juha-Pekka T. Huhtanen
Department of Energy and Process Engineering, Tampere University of Technology
PO Box 589, FIN-33101 Tampere, Finland
mika.piirto@tut.fi, juha-pekka.huhtanen@tut.fi

ABSTRACT

This paper introduces a comparison between CFD simulations and experimental data of a dilute fibre suspension of bleached softwood chemical pulp fibres in a backward facing step channel flow. Average velocities and turbulence quantities are measured with Particle Image Velocimetry (PIV) technique in pure water and in 0.2 mass-% suspension flow, and the results are compared with numerically modelled data. Different mechanisms of the modification of turbulence are studied and, based on a theoretical review, an extra dissipation term is added to Reynolds stress turbulence model (RSM) to simulate the effect of fibres on turbulent quantities. The attenuation of turbulence in the step area and the shift of reattachment point further downstream after abrupt expansion is well captured by the presented model.

INTRODUCTION

Many unit processes in the pulp and paper industry are based on turbulent fibre-water suspension flows. Better understanding of the effect of suspended solid matter on the flow properties of the carrier phase is important in order to control the process accurately in different operating conditions. Because of the large aspect ratio (*l/d*) of fibres, strong particle interactions occur in fibre-water flow even at low consistencies ($c \gtrsim 0.1$ %). As a consequence, the fibres move as flocks and the fibre and floc interactions cause a feedback on turbulence structure. Extensive reviews of the observations and flow properties in turbulent fibre suspension have been presented by Parker (1972), Norman *et al.* (1977) and Kerekes *et al.* (1985). However, scarce quantitative information exists about turbulence modification and characteristics in fibre suspensions due to the complexity of measurements as well as modelling.

The main interest around turbulence measurements is to explain the changes in turbulence structure due to the presence of solid matter in suspension. A great deal of theoretical and experimental information exists in the literature about the reduction or increase of the turbulence intensity caused by the presence of spherical particles in a fluid (Yuan & Michaelides 1992, Hetsroni 1989). An extensive review of Gore and Crowe (1989) showed that small particles ($d_p < 0.1l'$ where l' is the length scale of turbulent eddies) will dampen turbulence due to the relative velocity induced drag effect, while larger particles tend to enhance turbulent kinetic energy due to vortex shedding in the wake of the particle.

Modified k-ε turbulence models including the effects described above have been developed and tested for dilute suspensions of spherical particles (Elghobashi & Abou-Arab 1983). However, since fibres are non-spherical and tend to form flocks, it is difficult to develop a rigid mathematical model analogue to the approach used in the dilute particle suspensions of spherical particles.

Most observations of turbulence in fibre suspensions have been reported by using the Laser Doppler Anemometry (LDA) technique in straight pipe flow. Several authors (Chuang 1982, d'Incau 1983) have reported reduced turbulent intensities in fibre suspensions compared to pure fluid flow. Ek (1979) measured reduced turbulent intensities in the core of the pipe in a $c = 0.5$ % fibre suspension compared to pure water flow while turbulent intensity was greater in the wall region. Steen (1989a,b) used different consistencies and fibre lengths concluding that kinetic energy decreased with increased consistency and fibre length.

Few attempts have been made to model turbulent fibre suspension flows (Hourani 1988a,b, Steen 1990). Steen (1990) has presented a model for Fibre Flocculation Concept where the fibrous phase is described with a new variable, flocculation intensity. The model is based on single-phase description where an additional scalar transport equation is solved for flocculation intensity and the effects of fibres on momentum and turbulence equations are neglected.

The objective of this study is to provide a straightforward way to model turbulence in dilute ($c = 0.2$ %) fibre-water suspension flow. Fibre effected turbulence modification is

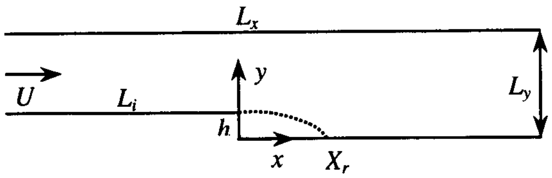

Figure 1. Schematic picture of the flow domain.

based on the idea of an extra dissipation term in turbulent shear stress components in RSM turbulence model due to the energy needed for suspension fluidisation. The presented model is tested in channel flow over a backward facing step and the simulation results are compared with PIV measurements carried out in the same geometry (Piirto *et al.* 2003).

EXPERIMENTAL SETUP

Figure 1 shows a schematic view of the flow domain used both in measurements and in simulations. The examined domain consisted of total stream-wise length $L_x = 90h$ with an inlet section $L_i = 55h$ prior to the sudden expansion. Vertical height was $L_y = 4h$ after the expansion and the span-wise width of the channel was $L_z = 2h$, where h is the step height. The coordinate system was placed at the lower step corner as shown in Figure 1. The step-height Reynolds number for water was defined as $Re_h = U_0h/\nu \approx 36\ 500$, where U_0 is the maximum mean inlet velocity. The expansion ratio was $ER = L_y/(L_y - h) = 1.33$.

Due to the operation principle of PIV, based on laser sheet optics and a CCD camera, the measurement of a suspension flow required special efforts. The penetration of a laser light sheet in fibre suspension was limited leading to incomplete image capturing deeper in the flow domain. Thus, the intensity of images decreased towards the middle part of the channel, but this phenomenon did not directly affect the location of the velocity vector correlation peaks, i.e. calculated displacement did not depend on the image intensity (Piirto *et al.* 1999). However, especially in the middle part of the channel, the noise in the image capturing may have increased the velocity random error, and thus the error in turbulence characterisation. Generally, the random error incorporated with the PIV system and iterative discrete interrogation algorithm (Westerweel *et al.* 1997) was of the order 0.05-0.1 pix leading to the non-dimensional measurement r.m.s. error of the order 0.01-0.02.

In addition to the visible fibres, the flow was seeded by polyamide particles with an average size of 5 μm. The seeding particles were needed only in the lower part of the channel where the fibre concentration was lower due to phase separation. In the middle part of the channel seeding particles had no practical meaning since fibres and flocks were dominating the flow. PIV as a method does not separate the motion of seeding particles and fibres, and thus the computed velocity field was composed of average displacements of seeding particles and fibres in each interrogation area. In the processing of velocity vectors, very few erroneous vectors were found when the correlation

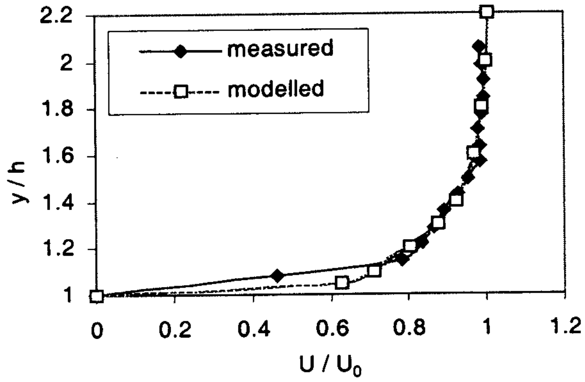

Figure 2. Measured and modelled average velocity profile for water just before the step (x/h = 0).

peaks were required to be located in the allowed velocity range. The measurement resolution was $0.08h$ and the size of the interrogation area was $0.08h \times 0.08h$ (32×32 pix).

Reynolds stress components and mean velocity profiles at locations $x/h = 4$, $x/h = 6.5$, $x/h = 9$ and $x/h = 17$ were computed from the PIV data and compared with the results of the simulations described below. In addition, the PIV results were compared with Direct Numerical Simulation (DNS) data of Le *et al.* (1997) and experiments conducted by Jovic & Driver (1994) in order to validate the measurements in general terms. However, it should be noticed that backward-facing step flows studied by Le *et al.* and Jovic & Driver had lower Re_h than presented here, even though ER and reattachment length X_r were almost the same.

Numerical modelling work was carried out with the commercial CFD code Fluent 6.0.20. Although the actual flow field in the examined domain is certainly 3-dimensional, the simulations were carried out in a 2d-domain in order to get a fine enough grid with moderate calculation time. The position of the reattachment was found to be very sensitive for grid properties, and after ca 60 000 cells further grid refinement did not result in significant chances in reattachment behaviour. An RSM turbulence model with default model constants (Fluent Inc. 2001) and 10^{-4} convergence criteria for all variables was used.

The mean inflow velocity profile $U(y)$ imposed at the inlet boundary in simulations was taken from PIV measurements. Measured and modelled profiles for water just before the step are shown in Figure 2. Setting of correct boundary conditions for inlet turbulence quantities before the step was complicated since appropriate measurements were not available. Constant 10 % turbulent intensity was set to the inlet and turbulent quantities were assumed to have enough time to develop prior to the sudden expansion. However, before the measured flow domain there was a shape change from circular pipe to rectangular channel, and the inlet section L_i appeared to be too short for the flow field to be considered as fully developed before the step. This may cause some inaccuracy when measured and modelled absolute values are compared with each other, especially with respect to turbulent quantities. However, the trends between water and suspension behaviour in measurements and in simulations are well comparable.

THEORY AND MODELS

Most of the models for turbulent flow including solid matter are based on an assumption of very dilute suspension of spherical particles without bilateral collisions (Elghobashi & Abou-Arab 1983). However, fibre suspensions behave differently from dilute particle suspensions since fibres interact with each other and form flocks even at low consistencies, and the internal fibre network resists a certain yield stress, τ_y (Bennington et al. 1990). In general, Yuan and Michalides (1992) have summarised six mechanisms that may modify the turbulence structure in particulate flows:

1) Dissipation of kinetic energy caused by the particles
2) Increase of the apparent viscosity due to the particles
3) Shedding of vortices or the presence of wakes
4) Fluid moving with the particle as added fluid mass
5) Enhancement of velocity gradients between particles
6) Deformation of the dispersed phase

For dilute fibre suspension flow with small density difference between the phases, mechanisms 1 and 2 are most significant. Increased dissipation leads to the attenuation of turbulence and affects to momentum transport through the changes in turbulent viscosity. Increased apparent viscosity simply enhances the diffusion in the transport equations of momentum and turbulent quantities. At the laminar region fibre suspension is proposed to flow as a continuum non-Newtonian Bingham fluid with a shear dependent viscosity:

$$\mu_a = \tau_y / \dot{\gamma} + \mu_p \qquad (1)$$

where μ_a is apparent molecular viscosity, $\dot{\gamma}$ shear rate and μ_p plastic viscosity, which for dilute suspension can be defined as the apparent molecular viscosity of the carrier fluid, i.e. water. Thus at low shear rates suspension apparent viscosity approaches infinity while at high shear rates it approaches water viscosity. In addition to increased Bingham viscosity, Steen (1993) has proposed an added apparent viscosity due to flock collisions analogue to the Bagnold (1954) model for dense suspension of spherical particles. However, this issue is not considered here because of the low concentration of fibres. In transition or low turbulence region the momentum transfer is determined by effective viscosity, which is a sum of apparent molecular and turbulent viscosity. In fully turbulent flow, as in question here, the momentum transfer is supposed to be totally controlled by turbulent viscosity and the non-Newtonian effect of apparent viscosity can be neglected.

It is supposed here that the dissipation of turbulent kinetic energy arises from the work continuously needed to break up local flocks, i.e. the dissipation is equal to the energy required for suspension continuous fluidisation. Many authors have studied the fluidisation phenomenon in fibre suspension flows (Bennington & Kerekes 1996, Gullichsen & Härkönen 1981) and concluded that after a certain shear level, the suspension is in a turbulent state and exhibits properties commonly associated with Newtonian fluid. After fluidisation the suspension momentum transport is controlled by turbulent viscosity rather than by apparent

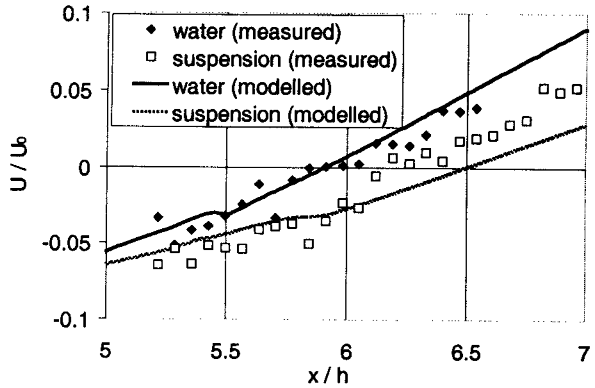

Figure 3. Measured and modelled reattachment point for water and for suspension (y/h = 0.05).

molecular viscosity. Bennington and Kerekes (1996) assumed that suspension fluidisation occurs when the local shear stress of fluid is everywhere equal to the yield stress of the fibre network, τ_y (the stress required to initiate the flow under shear), and certain energy proportional to τ_y is required for the onset of fluidisation. It is further proposed that this yield stress-related amount of energy is continuously dissipated from local turbulent shear stress in order to maintain the fluidisation.

In the RSM model the production of stress components is expressed by multiplying Reynolds stresses by mean velocity gradients. The dissipation term is expressed similarly to standard k-ε model: normal Reynolds stress components are multiplied by "turbulent shear rate" ε/k. Supposing that the basic production and dissipation mechanisms remain unchanged in dilute turbulent fibre suspension flow, an additional dissipation term to turbulent shear stress equation can be defined as:

$$\varepsilon_e = \varepsilon\tau_y / k \qquad (2)$$

The magnitude of suspension yield stress depends on fibre properties and mean consistency and has been broadly studied in literature (Bennington *et al.* 1990, Bennington & Kerekes 1996, Huhtanen 1998). In this case, τ_y is assumed to be of the order 20 Pa (c = 0.2 %, $l/d \approx 60$). The equations of turbulence kinetic energy and dissipation in the RSM model are remained unchanged, and the modified transport equation for Reynolds stresses is presented below (Eq. 3):

$$\underbrace{\frac{\partial\left(\rho u_k \overline{u'_i u'_j}\right)}{\partial x_k}}_{convection} = \underbrace{p\overline{\left(\frac{\partial u'_i}{\partial x_j}+\frac{\partial u'_j}{\partial x_i}\right)}}_{pressure\ strain} + \underbrace{\frac{\partial}{\partial x_k}\left[\left(\mu_a+\frac{\mu_t}{\sigma_k}\right)\frac{\partial\left(\overline{u'_i u'_j}\right)}{\partial x_k}\right]}_{molecular\ \&\ turbulent\ diffusion} \qquad (3)$$

$$- \underbrace{\rho\left(\overline{u'_i u'_k}\frac{\partial U_j}{\partial x_k}+\overline{u'_j u'_k}\frac{\partial U_i}{\partial x_k}\right)}_{stress\ production\ P_{ij}} - \underbrace{\frac{2}{3}\delta_{ij}\rho\varepsilon}_{dissipation\ \varepsilon_{ij}} - \underbrace{(1-\delta_{ij})\rho\varepsilon_e}_{extra\ dissipation}$$

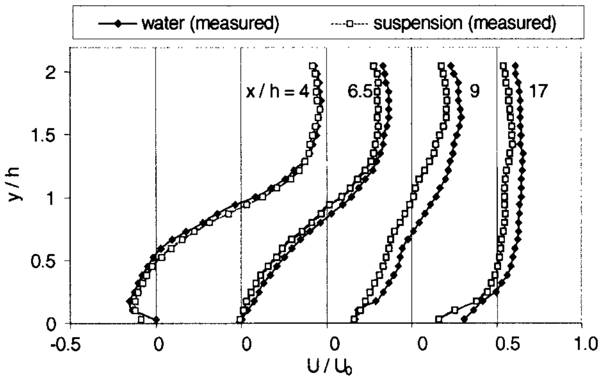

Figure 4. Measured average velocity profiles for water and for suspension at different axial positions.

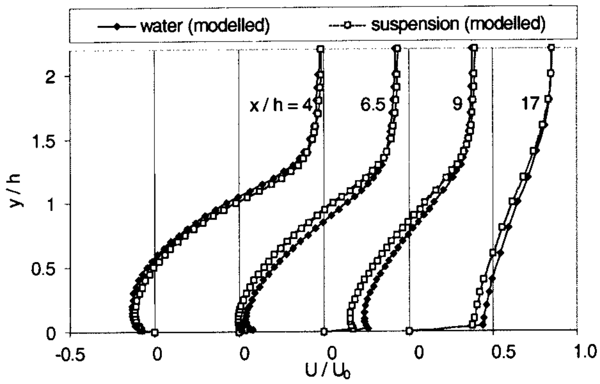

Figure 5. Modelled average velocity profiles for water and for suspension at different axial positions.

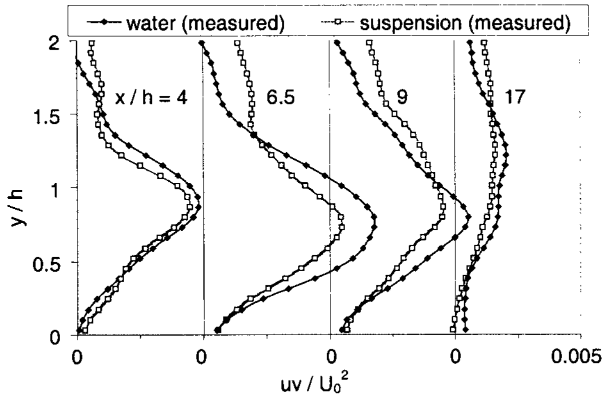

Figure 6. Measured uv profiles for water and for suspension at different axial positions.

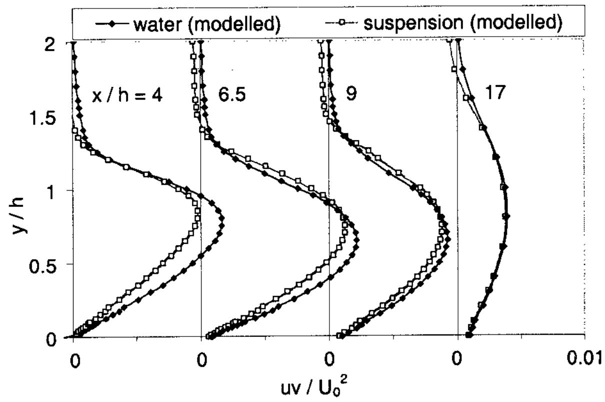

Figure 7. Modelled uv profiles for water and for suspension at different axial positions.

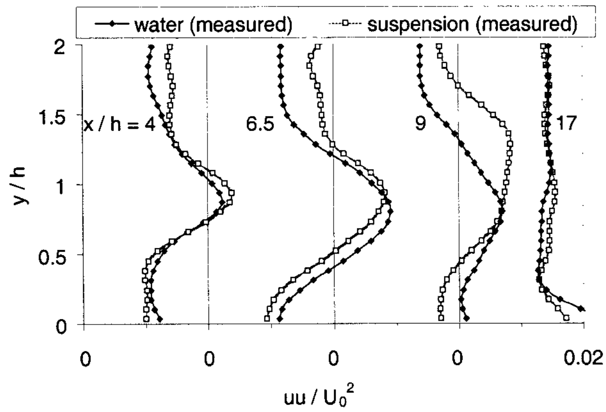

Figure 8. Measured uu profiles for water and for suspension at different axial positions.

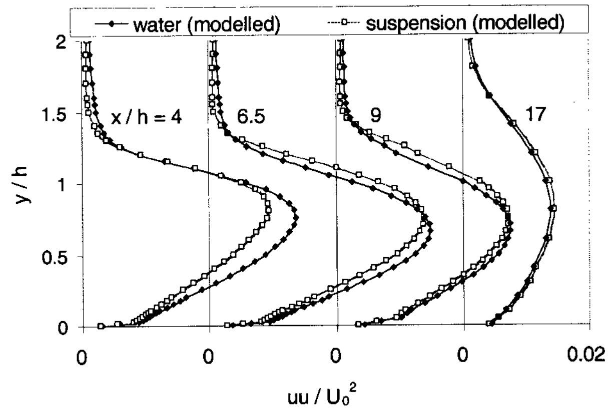

Figure 9. Modelled uu profiles for water and for suspension at different axial positions.

where U_i and u_i' are the mean and fluctuating velocity components respectively, p the pressure, μ_a and μ_t apparent molecular and turbulent viscosity respectively, and ρ the density. The subscripts i,j,k take the values 1,2 to denote the streamwise (x) and vertical (y) directions respectively.

RESULTS AND DISCUSSION

Measured and simulated axial velocities close to the step wall for water and for suspension are shown in Figure 3. It can be seen that the RSM turbulence model correctly predicts the reattachment of water flow after step even though the calculations were carried out in 2d. The reattachment point for water in PIV measurements and in the

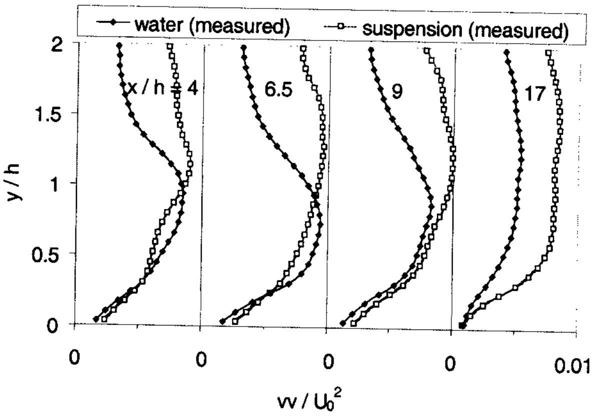

Figure 10. Measured vv profiles for water and for suspension at different axial positions.

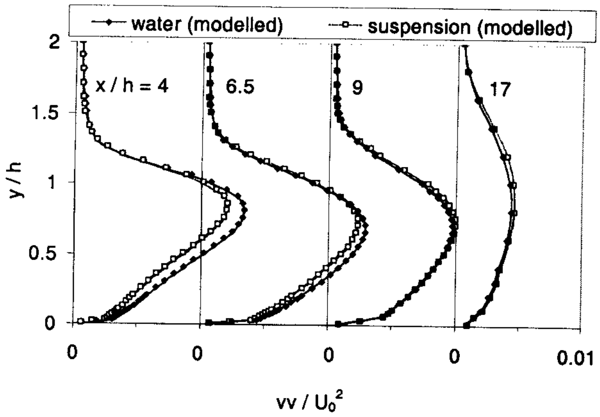

Figure 11. Modelled vv profiles for water and for suspension at different axial positions.

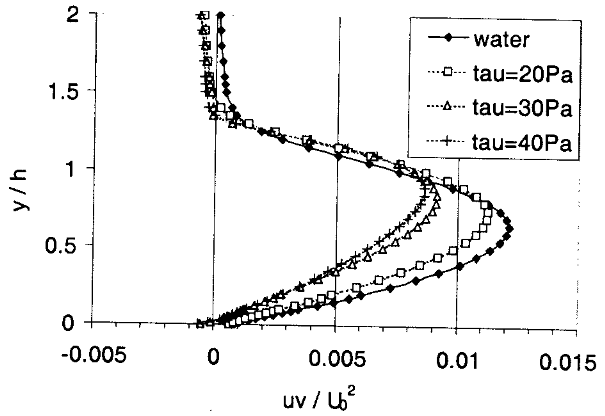

Figure 12. Effect of increasing yield stress on uv profile at x/h = 6.5.

presented RSM simulations was $X_r = 5.91h$. In the DNS data of Le *et al.* (1997) the reattachment occurred further downstream at $X_r = 6.28h$, but the values still are fairly close to each other.

Addition of fibres to the water clearly shifts the reattachment point further downstream both in measurements and in simulations, but the effect seems to be stronger in simulations. This may arise from too low effective viscosity in momentum equations since increasing apparent viscosity tends to move the reattachment closer to the step. A slight difference between simulations and measurements can also be explained with phase separation after an abrupt step, which is not taken account in the model.

Measured and modelled average velocity profiles for suspension and for water at different axial positions after the step are shown in Figures 4-5. Despite the 2d-simplification, the RSM turbulence model for water captures well the mean velocity developing after a sudden expansion when compared to water measurements. It can be seen that in PIV measurements the general shape of the axial velocity profile at distances x/h = 9 and 17 is too flat when compared to simulations and to data presented by Le *et al* (1997).

In the modified RSM model the behaviour of suspension average velocity is predicted correctly at the step area, where the presence of fibres tends to reduce the mean axial velocity. In the middle of the channel measured average velocity for suspension is lower than the simulated one. This indicates that the effective viscosity in momentum equations should be higher at low shear rate area, which might be handled by adding non-Newtonian behaviour to apparent viscosity. This decrease in mean velocity due to added fibres demonstrated in these measurements and simulations is also reported by Steen (1993) in straight pipe flow, albeit his model gave profiles that were too far flat compared to measurements.

Measured and modelled Reynolds stress (*uv*, *uu* and *vv*) profiles after the step for suspension and for water are shown in Figures 6-11. There is a clear difference in the magnitude of water *uv*-profiles in PIV experiments as compared to RSM simulations and to the results of Le *et al.* This is explained as being due to undeveloped turbulence in the inflow of PIV measurements leading to too low shear stress values after the step (Piirto *et al.* 2003). The same kind of difference in magnitude is not observed so clearly between measured and modelled *uu* and *vv* profiles. However, the shape of the measured shear stress profiles for water is consistent with the DNS data of Le *et al.* and with simulated profiles presented here, whereupon the Reynolds stress values between PIV measurements and simulations can be compared qualitatively but not quantitatively.

At the step area in Figures 6-7, the direction and magnitude of chance in *uv* level between water and suspension is the same both in measurements and in simulations: added dissipation term decreases the maximum value of the Reynolds stress *uv* component. Simulated *uu* and *vv* profiles in Figures 9 and 11 indicate the same behaviour: attenuation of maximum value, which is earlier reported to happen for turbulent kinetic energy, too (Steen 1990, Chuang 1982, d'Incau 1983, Ek 1979). In contrast to PIV measurements, the simulations predict approximately equal or lower shear and normal stress values for suspension compared to water in the middle part of the channel at all axial distances. Furthermore, in simulations at the distance x/h = 17, no remarkable difference is observed between water and suspension *vv* profiles like in the measurements. These departures may be the result of inaccurate inlet turbulence boundary conditions as well as possible 3-dimensional effects ignored in the 2-dimensional model. Despite a moderately high Reynolds number, the impact of higher apparent molecular viscosity at a low shear rate area (i.e. in the middle of the channel) is an important factor not taken into account in the presented model. These issues should be studied further with more precise measurement arrangements having fully developed inlet conditions before the step.

The effect of increasing yield stress on the turbulent shear stress profile is presented in Figure 12. The magnitude of yield stress in extra dissipation term is increased from 20 to 40 Pa while other model parameters are kept constant. As expected, increasing τ_y in the extra dissipation term increases the effects described above. However, it should be kept in mind that, despite the attenuating turbulence, the flow still has to remain at a fully turbulent regime for the model assumptions to be valid.

CONCLUSIONS

A turbulent fibre suspension model with a simple additional dissipation term was tested in channel flow over a backward facing step. Average velocities and turbulence quantities for water and for suspension were compared with PIV measurements and earlier data. The attenuation of turbulence at the step area and the shift of the reattachment point further downstream after abrupt expansion was well captured by the presented model. However, some departures were observed between measured and simulated turbulence quantities in the middle part of the channel where mean shear rate is low. Combining the modified turbulence model with non-Newtonian viscosity properties, especially in turbulent flows with lower Reynolds number, is an issue to be studied in more detail.

In general, the results obtained with a simple modified RSM model were promising, and the usefulness of the model should be further tested with different consistencies and more complicated geometry.

REFERENCES

Bagnold, R. A., 1954, "Experiments on a gravity-free dispersion of large solid spheres in a newtonian fluid under shear," Proc. Royal Society London, A225, pp. 49.

Bennington, C. P. J., Kerekes, R. J., and Grace, J. R., 1990, "The yield stress of fibre suspensions," *Can. J. of Chem.* Eng., Vol. 68, pp. 748.

Bennington, C. P. J., and Kerekes, R. J., 1996, "Power requirements for pulp suspension fluidization," *Tappi J.*, Vol. 79:2, pp. 253-258.

Chuang, S. C., 1982, "Microturbulence generation in a papermachine headbox," *Tappi Eng. Conference*, San Francisco, California, pp. 205.

d'Incau, S., 1983, "Characterization of the decay of turbulence in a pulp suspension flow," *Tappi Eng. Conference*, Dallas, Texas, pp. 583.

Ek, R., 1979, "Simultaneous measurements of velocity and concentration in fiber suspension flow," *Int. Symposium on Paper Machine Headboxes*, McGill University, Montreal, Canada, pp. 31.

Elgobashi, S. E., and Abou-Arab, T. W., 1983, "A two-equation turbulence model for two-phase flow," *Phys. of Fluids*, Vol. 26:4, pp. 931.

Fluent User's Guide, version 6.0, 2001, Fluent Incorporated, Lebanon.

Gore R. A., and Crowe C. T., 1989, "Effect of particle size on modulating turbulent intensity," *Int. J. Multiphase Flow*, Vol. 15:2, pp. 279-284.

Gullichsen, J., and Härkönen, E., 1981, "Medium consistency tehchology," *Tappi J.*, Vol. 64:6, pp. 69-72.

Hetsroni G., 1989, "Particles-turbulence interaction," *Int. J. Multiphase Flow*, Vol. 15:5, pp. 735-746.

Hourani, M. J., 1988a, "Fiber flocculation in pulp suspension flow Part 1: Theoretical model," *Tappi J.*, Vol. 71:5, pp. 115-118.

Hourani, M. J., 1988b, "Fiber flocculation in pulp suspension flow Part 2: Experimental results," *Tappi J.*, Vol. 71:6, pp. 186-189.

Huhtanen, J-P., 1998, "Non-Newtonian flows in paper making," Licentiate Thesis, Tampere University of Technology, Energy and Process Engineering, Finland.

Jovic, S., Driver, D.M., 1994, "Backward-facing step measurement at low Reynolds number, Re_h = 5000," *NASA Tech. Mem.* 108807.

Kerekes, R. J., Soszynski, R. M., and Tam Doo, P.A., 1985, "The flocculation of pulp fibres," *Papermaking raw materials, The 8th Fundamental Research Symposium*, Oxford, UK, pp. 265.

Le H., Moin P., and Kim J., 1997, "Direct numerical simulation of turbulent flow over a backward facing step," *J. Fluid Mech.*, Vol. 330, pp. 349-374.

Norman, B. G., Møller, K., Ek, R., and Duffy, G.G., 1977, "Hydrodynamics of papermaking fibers in water suspensions," *Fiber-Water Interactions in Papermaking. The 6th Fund. Research Symp.* Oxford, UK, pp. 195.

Parker, J. D., 1972, "The sheet forming process," *Tappi STAP*, No. 9, Atlanta, Georgia.

Piirto M., Saarenrinne P., 1999, "Interaction between flocculation and turbulence – A method using the combination of image processing and PIV," *3rd ASME/JSME Joint Fluids Engineering Conference*, San Francisco, California, USA.

Piirto, M., Saarenrinne, P., Eloranta, H., and Karvinen, R., 2003, "Measuring turbulence energy with PIV in a backward-facing step flow," *Exp Fluids*, to be published.

Steen, M., 1989a, "On turbulence structure in vertical pipe flow of fiber suspensions," *Nordic Pulp & Paper Research J.* Vol. 4:4, pp. 224.

Steen, M., 1989b, "The application of refractive index matching for two-phase flow measurements in turbulent fiber suspensions by laser doppler anemomertry," *Nordic Pulp & Paper Research J.* Vol. 4:4, pp. 236.

Steen, M., 1990, "Turbulence and flocculation in fibre suspensions," The University of Trondheim, Division of Thermodynamics, dissertation, pp. 86.

Steen, M., 1993, "On turbulence and flocculation in fiber suspensions," Institute of Paper Science and Technology, Atlanta, Georgia.

Westerweel, J., 1997, "The effect of a discrete window offset on the accuracy of cross-correlation analysis of digital PIV recordings," *Exp. Fluids*, Vol. 23, pp. 20-28.

Yuan, Z., and Michaelides, E. E., 1992, "Turbulence modulation in particulate flows – a theoretical approach," *Int. J. Multiphase Flow*, Vol. 18:5, pp. 779-785.